Investigation of using BSPT for ring-dot piezoelectric transformers for use in high-temperature resonant power supplies

Jack Forrester, Linhao Li, Jonathan N. Davidson, Martin P. Foster, David A. Stone, Ian M. Reaney
Derek C. Sinclair
University of Sheffield
Sir Frederick Mappin Building, Mappin Street
Sheffield, S1 3JD
Ph: 0114 222 5392
Email: jack.forrester@sheffield.ac.uk

Abstract

SiC and GaN devices are gaining in popularity in both research and commercial applications. One of the many benefits of these devices is the possibility of power converter operation at temperatures in excess of that possible with Si-based devices (>200°C). A bismuth scandium lead titanate (BSPT) piezoelectric transformer is analysed for use in high temperature (up to 250°C), resonant converters using impedance spectroscopy and power converter measurements. The PT shows declining losses with temperatures during testing, translating into an improvement of 15% points in efficiency whilst more than doubling the output power across the temperature range. A peak performance of 0.7W output power and 53% efficiency at 225°C was achieved, giving comparable performance to previous work but at higher temperatures.

Key words

High Temperature, Piezoelectric Transformers, Resonant Converters, Zero Voltage Switching

I. Introduction

Piezoelectric transformers (PT) conveniently replace many of the discrete components within a resonant power supply. PTs high power density, high efficiency and inherent resonant tank make them ideal for low to medium (<50W) resonant converter applications. One of the advantages of PTs is that piezoelectric materials can operate in harsh environments, such as in high temperatures and high magnetic fields. This makes piezoelectrics ideal for used in one of several emerging high temperature power electronic applications [1], [2]

Researchers have developed individual high temperature passive electronic components that can operate at temperatures of up to 200°C [3], [4]. However, when constructing a full converter based on high temperature components, a 55% efficiency at 1W and about 65% efficiency at 2W was achieved at a temperature of 200°C [5]. High temperature passive electronic components are more complex to design and offer inferior performance compared to low temperature passives [6].

Whilst lead zirconium titanate (PZT) is the most popular and performant piezoelectric material used for high power PT applications, its comparatively low curie temperature (386°C) limits its maximum operating temperature. Bismuth scandium lead titanate (1−x)$BiScO_3$-x$PbTiO_3$ (BSPT) has been shown to exhibit a morphic phase boundary around x = 0.64 between the tetragonal ($PbTiO_3$) and rhombohedral ($BiScO_3$) phase regions [7]–[10]. BSPT-64 in particular exhibits excellent piezoelectric properties, including a high piezoelectric coefficient, coupling factors and importantly a higher curie temperature than state-of-the-art PZT materials (450°C), making this variant of BSPT potentially ideal for high temperature PT applications. For that reason, we will refer to BSPT-64 merely as BSPT throughout this paper.

The aim of this paper is to demonstrate the effectiveness of BSPT as a material for high temperature PTs for use in resonant power supplies for low power (<5W) applications. An analysis is performed investigating both the small and large signal performance of the PT and a PT based converter respectively. The equivalent circuit components of the PT are extracted from the impedance measurements, giving insight into how the performance of the PT changes with changes in temperature. Finally, an inductorless half bridge inverter is constructed, and its performance measured using a variety of metrics to determine the suitability of BSPT PTs for high temperature applications.

II. Converter Design

To evaluate the performance of a BSPT PT for use in resonant converters at high ambient temperatures, a suitable choice of PT and converter topology should be made. Once the topologies have been chosen, a suitable PT design will be formulated to enable exemplar performance at high ambient temperatures.

A. Converter topology

An inductorless half bridge converter was chosen for this application. A schematic for this inverter is shown in Fig. 1 below. The PT is replaced in the diagram by its Mason equivalent circuit, as shown in the dash box in Fig. 1. This converter topology was chosen due to its popularity, which is due to it requiring no additional magnetic components to allow zero voltage switching (ZVS) and thereby significantly reducing MOSFET switching loss [11].

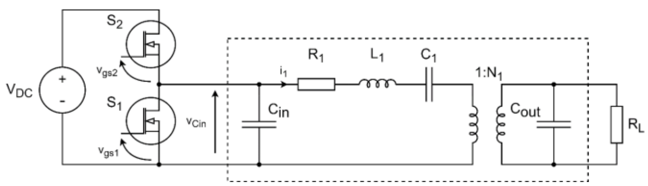

Fig. 1 - Inductorless half-bridge piezoelectric transformer resonant power supply, dashed line showing the Mason equivalent circuit

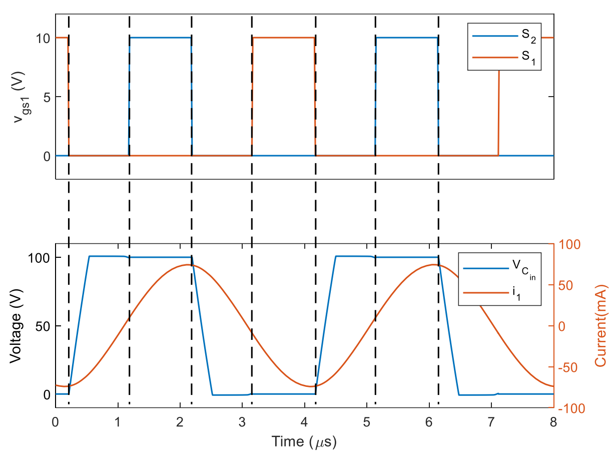

Fig. 2 - Waveforms for the inductorless half-bridge piezoelectric transformer resonant power supply

The inductorless half bridge operates by switching MOSFETs S_1 and S_2 in anti-phase with a 25% duty cycle, giving a 25% deadtime between switching operations. During the deadtime interval S_1 and S_2 are off, and so the resonant current i_1 charges $v_{C_{\text{in}}}$ from 0 to V_{DC} (or V_{DC} to 0) with a cosine waveshape. The analysis described in [12] provides guidelines for the ratio of input to output capacitance and deadtime interval duration necessary to achieve ZVS, thereby avoiding unnecessary switching losses in the MOSFETs. The resulting input voltage to the PT is of trapezoidal shape, as shown in the waveforms in Fig. 2.

Given the high Q factor (>50) typically exhibited by the PT's inherent resonant tank circuit, the harmonics in the trapezoidal-like waveform are filtered causing the resonant current to be approximately sinusoidal. Thus, the output voltage of this converter is a high frequency sinusoid. Additional rectification and filtering could be added; however, it has been omitted here.

B. PT topology and design

A ring-dot PT topology was chosen, due to its simplistic construction compared to other high power PT topologies. The ring-dot is made from a single layer of piezoelectric with concentric ring (output) and dot (input) shaped electrodes on the upper face and ground electrode on the lower face, shown in Fig. 3.

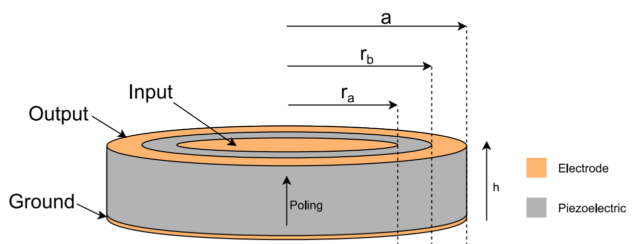

Fig. 3 - Ring-dot PT

For this application, a ring-dot PT with radius (a) of 8mm, a thickness (h) of 1.1mm, an $r_a = 3.4$mm and an $r_b = 5.7$mm was chosen. The radius and thickness were chosen to achieve a radius/thickness ratio of approximately 7, ensuring that the PT avoids interaction with spurious modes [13]. Foster et al. developed a criterion that states that for this converter topology, if the capacitance ratio $(C_N = C_{\text{in}}/N^2C_{\text{out}})$ is designed to be $< 2/\pi$, then ZVS can be achieved irrespective of the load (assuming correct driving conditions are met and efficient operation) [12]. Therefore, r_{a} and r_{b} were then chosen to achieve a capacitance ratio of 0.31 (measured at room temperature), ensuring the PT agrees with the criterion and by ensuring C_N is much less than $2/\pi$ provides some degree of tolerance regarding the efficiency of the PT. The PT is shown in Fig. 4 was manufactured in-house using BSPT material.

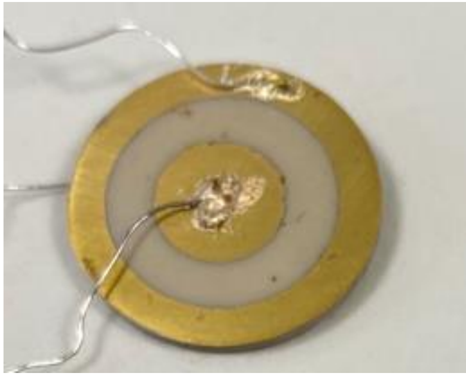

Fig. 4 - Prototype BSPT PT

III. Testing Procedure

To evaluate the performance of the BSPT at high ambient temperatures, both small-signal and large-signal testing was performed. Small signal impedance measurements were taken using an Omicron Bode 100, from both the input and output terminals, with the non-driven terminal short circuited to ground. Then, using these impedance measurements and leveraging the extraction method presented by [14], the Mason equivalent circuit properties can be estimated, giving insight into the PTs performance at a range of temperatures. Secondly, an inductorless half bridge inverter is constructed based on this device. The phased-locked loop ZVS controller presented by [15] was used to ensure the converter was operating at the resonant frequency to maximize the ZVS capability and, thus, minimize losses. The large-signal measurements used for determining output power and efficiency were obtained using a Yokogawa power scope. Similarly, the input power to the PT was also measured under the same driving conditions, allowing the losses in the converter to be allocated to the MOSFETs and the PT. During the experiments, ideally a matched load ($R_L = 1/\omega C_{\mathrm{out}}$) should be used to maximise PT and converter efficiency. However, the results of the small-signal experiment demonstrated that both resonant frequency and output capacitance change with temperature making it difficult to determine the exact matched load. Therefore, a 1kΩ, a 500Ω and a 220Ω loads were used during the large-signal experiments and the load that provided the greatest efficiency is presented here.

In both sets of experiments, only the PT was placed within a small tube furnace, allowing the ambient temperature to be controlled. The PT hung freely within the furnace, allowing minimal vibration damping from the experimental setup, shown in Fig. 5. The ambient temperature was varied between 25-250°C in 25°C increments. Before each measurement, the temperature was allowed to settle and then left for 20 minutes to ensure the PT was at the measured temperature. The temperature was measured using a thermocouple placed within 1cm of the PT. Electrical connections were run though a ceramic rod (used to hold the PT in place) allowing connections to be made outside of the furnace.

Fig. 5 - PT hanging from ceramic rod in furnace

C. Small-Signal Experiment

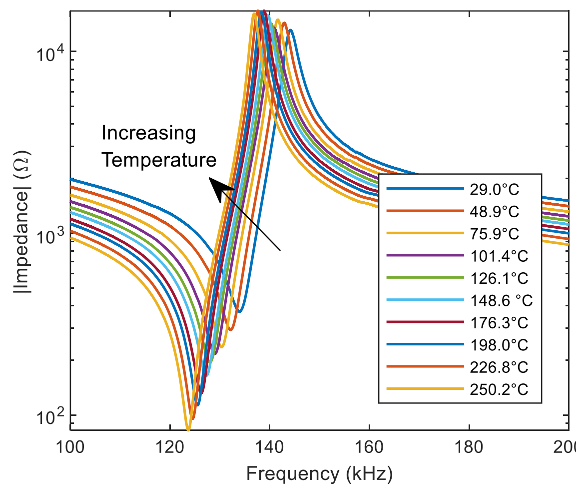

a)

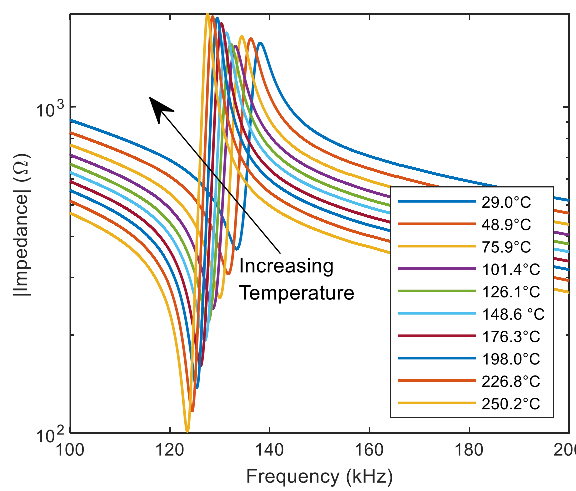

b)

Fig. 6 - Measured impedance spectra, (a) input impedance (output shorted) (b) output impedance (input shorted)

Fig. 6 shows the input (a) and output (b) impedance spectra of the PT measured at various ambient temperatures. The results show a notable change in impedance magnitude, resonant and anti-resonant frequencies can be observed. Using the techniques described in [14] the Mason equivalent circuit components were extracted.

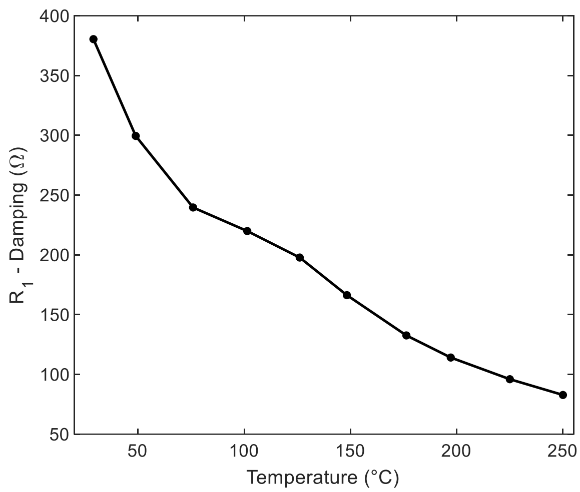

Fig. 7 - Damping resistance R_1

By way of example, Fig. 7 shows the change in damping resistance R_1 with changes in ambient temperature. At room temperature, the BSPT PT exhibits a very high damping of 380Ω. However, as the temperature increases, a significant decrease in damping resistance can be observed. At 250°C a damping resistance of 83Ω was observed showing an almost five-fold decrease in damping across the temperature range. The reduction in damping is vital for converter performance, as it is this equivalent resistance that is responsible for the majority of the losses in the converter and thus a significant in improvement in efficiency should be observed with increases in temperature.

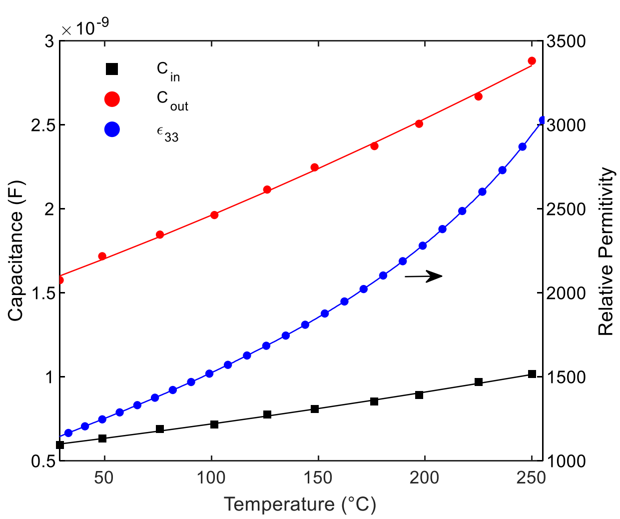

Fig. 8 - Input (C_{in}) and output (C_{out}) capacitance, and ε_{33}

Fig. 8 shows the change in input and output capacitance with changes in ambient temperature. In Fig. 8, both capacitances experience a notable increase in value with temperature. This is to be expected, as we can also observe an increase in relative permittivity with temperature for BSPT. Importantly, the ratio of input to output capacitance changes negligibly over the temperature range, so the PT will still meet the criterion set in [12]. However, as the output capacitance increases, the resonant current amplitude increases as a result, which leads to further losses in the PT ($i_1^2 R_1$) and thus lowered efficiency at higher temperatures [16].

D. *Large-Signal Experiment*

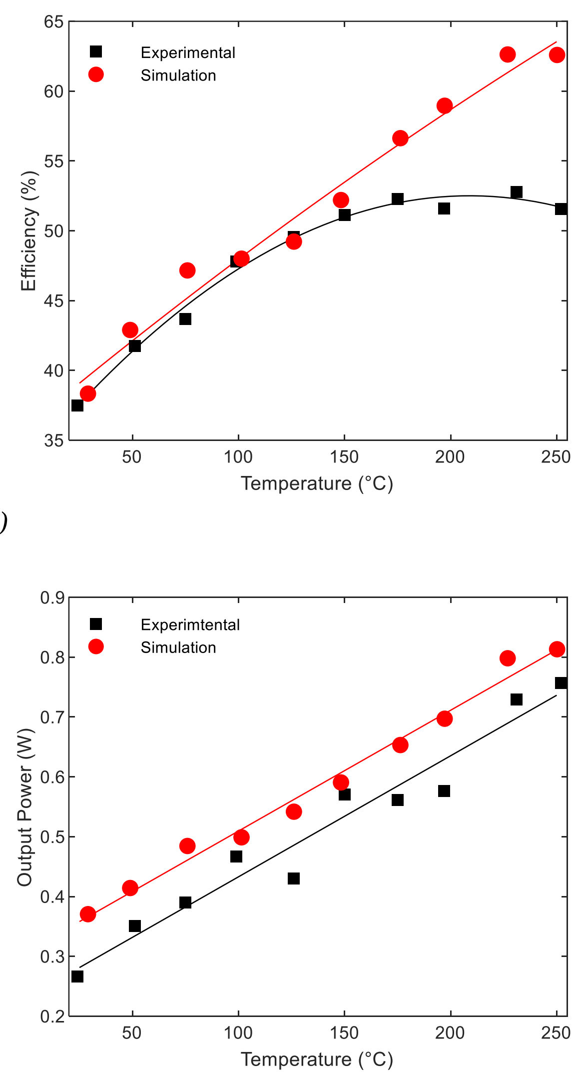

a)

b)

Fig. 9 - Inductorless half bridge inverter efficiency (a) and output power (b)

As suggested by the results in Fig. 7, Fig. 9 shows the inverter exhibits low (38%) efficiency at room temperature because of the very high damping exhibited by the PT. An additional consequence of the large damping value is the output power of the inverter is also low at 0.27W (80 V input). However, as the ambient temperature increases, the damping resistance reduces and notable increases in both efficiency and output power are achieved. The efficiency of the inverter peaks at 225°C with a value of 53% whilst achieving an output power of 0.73W.

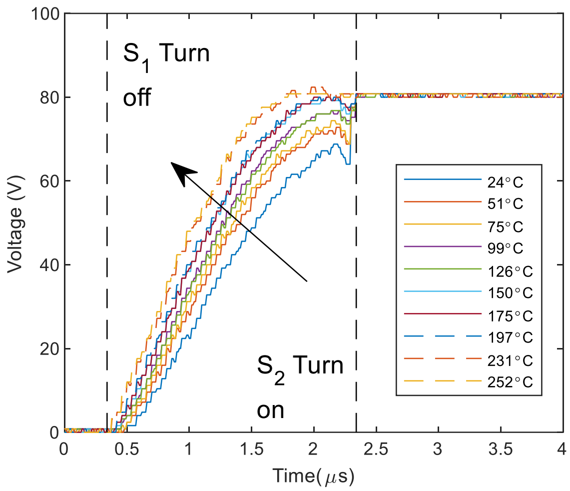

Fig. 10 - PT input waveform $V_{C_{in}}$, arrow indicating changes with increasing temperature

Fig. 10 shows the voltage waveform measured at the input to the PT (i.e. across the input capacitance) with changes in ambient temperature. During the S_2 turn-on deadtime interval, resonant current i_1 is negative, thus current flows in to C_{in} charging $v_{C_{\text{in}}}$ in a positive direction. At the end of the deadtime interval t=2.3μs, S_2 turns on connecting the PT to V_{DC}. ZVS is achieved if $v_{C_{\text{in}}} = V_{\text{DC}}$ when S_2 turns on. As can be seen when operating at high temperatures (>200°C) the PT clearly achieves ZVS. As the temperature reduces, the value of R_1 is sufficiently high to restrict the resonant current, limiting the charge available to change $v_{C_{\text{in}}}$. Therefore, the ability to achieve ZVS reduces and switching losses in the MOSFETs occur [12]. A similar waveform can also be observed during the deadtime between S_2 turn-off and S_1 turn-on.

Fig. 11 shows the power distribution in the converter as a function of temperature. As the temperature increases, a higher proportion of the input power is delivered to the load, as indicated in Fig. 9. Notably we observe a decrease in the losses in the MOSFETs. As output power (thus input power) increases with temperature, a proportional increase in conduction loss in the switches also occurs. Therefore, the decrease in MOSFET loss observed in Fig. 11 is predominantly due to the reduction in switching loss as expected based on measurements of $v_{C_{\text{in}}}$ presented in Fig. 10.

PT loss decreases with temperature but not much as expected based on the significant reduction in damping observed during small signal testing. It should also be noted that the PT loss is at least 3 times larger than the MOSFET loss across the whole temperature range. Therefore, improvements to the PT to lower the damping and the output capacitance would lead to significant improvements in inverter performance.

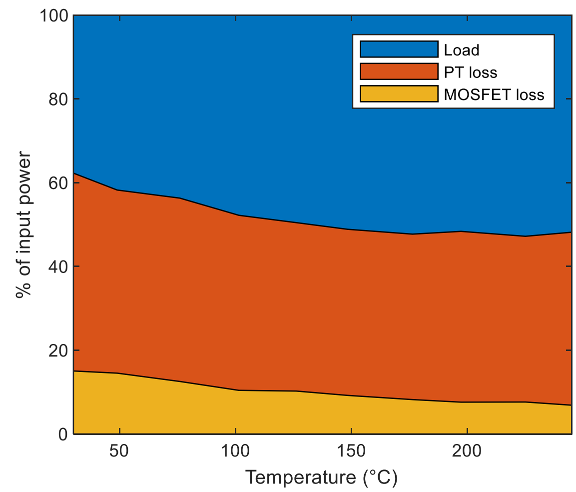

Fig. 11 - Power breakdown in the inductorless half bridge converter with a 500Ω load

IV. Conclusions

A suitability analysis for the use of BSPT based PTs for use in high temperature resonant power inverters is presented. A ring-dot PT was fabricated from BSPT material, with appropriate design for operation within an inductor less half bridge. An inductorless half-bridge PT inverter was constructed, and a series of measurements taken. The results presented here show an improvement in ZVS characteristics with temperature, with optimal performance at temperatures >200°C. Results obtained from a small-signal impedance characterisation shows a reduction in equivalent series resistance R_1 with temperature, explaining improvements in efficiency and ZVS that were observed during large signal testing. Further results including input to output capacitance ratio, efficiency and power distribution collected during this study were presented and demonstrate that BSPT is a suitable material for high temperature PT resonant power supply applications

Acknowledgement

We thank the EPSRC for funding (Targeted waveform enhanced plasma microreactor: Engineering Chemistry at the Interface of Microbubbles, EP/S031421/1).

References

[1] R. Normann, ‘First High-Temperature Electronics Products Survey 2005’, 2006. doi: 10.2172/889944.

[2] J. Watson and G. Castro, ‘A review of high-temperature electronics technology and applications’, *J. Mater. Sci. Mater. Electron.*, vol. 26, no. 12, pp. 9226–9235, Dec. 2015, doi: 10.1007/s10854-015-3459-4.

[3] T. Funaki *et al.*, ‘Power Conversion With SiC Devices at Extremely High Ambient Temperatures’, *IEEE Trans. Power Electron.*, vol. 22, no. 4, pp. 1321–1329, Jul. 2007, doi: 10.1109/TPEL.2007.900561.

[4] B. Ray, J. D. Scofield, R. L. Spyker, B. Jordan, and Sei-Hyung Ryu, ‘High temperature operation of a dc-dc power converter utilizing SiC power devices’, in *Twentieth Annual IEEE Applied Power Electronics Conference and Exposition, 2005. APEC 2005.*, Mar. 2005, vol. 1, pp. 315–321. doi: 10.1109/APEC.2005.1452944.

[5] R. Perrin, N. Quentin, B. Allard, C. Martin, and M. Ali, ‘High-Temperature GaN Active-Clamp Flyback Converter With Resonant Operation Mode’, *IEEE J. Emerg. Sel. Top. Power Electron.*, vol. 4, no. 3, pp. 1077–1085, Sep. 2016, doi: 10.1109/JESTPE.2016.2544346.

[6] F. Dubois *et al.*, ‘A high temperature ultrafast isolated converter to turn-off normally-on SiC JFETs’, in *2012 IEEE Energy Conversion Congress and Exposition (ECCE)*, Sep. 2012, pp. 3581–3588. doi: 10.1109/ECCE.2012.6342486.

[7] R. E. Eitel, C. A. Randall, T. R. Shrout, P. W. Rehrig, W. Hackenberger, and S.-E. Park, ‘New High Temperature Morphotropic Phase Boundary Piezoelectrics Based on Bi(Me)O3–PbTiO3 Ceramics’, *Jpn. J. Appl. Phys.*, vol. 40, no. 10R, p. 5999, Oct. 2001, doi: 10.1143/JJAP.40.5999.

[8] R. E. Eitel, C. A. Randall, T. R. Shrout, and S.-E. Park, ‘Preparation and Characterization of High Temperature Perovskite Ferroelectrics in the Solid-Solution (1-x)BiScO3–xPbTiO3’, *Jpn. J. Appl. Phys.*, vol. 41, no. 4R, p. 2099, Apr. 2002, doi: 10.1143/JJAP.41.2099.

[9] C. A. Randall, A. Kelnberger, G. Y. Yang, R. E. Eitel, and T. R. Shrout, ‘High Strain Piezoelectric Multilayer Actuators?A Material Science and Engineering Challenge’, *J. Electroceramics*, vol. 14, no. 3, pp. 177–191, Jul. 2005, doi: 10.1007/s10832-005-0956-5.

[10] S. Zhang, C. A. Randall, and T. R. Shrout, ‘Dielectric and Piezoelectric Properties of $BiScO_3$ -$PbTiO_3$ Crystals with Morphotropic Phase Boundary Composition’, *Jpn. J. Appl. Phys.*, vol. 43, no. 9A, pp. 6199–6203, Sep. 2004, doi: 10.1143/JJAP.43.6199.

[11] M. Ekhtiari, Z. Zhang, and M. A. E. Andersen, ‘State-of-the-art piezoelectric transformer-based switch mode power supplies’, in *IECON 2014 - 40th Annual Conference of the IEEE Industrial Electronics Society*, Oct. 2014, pp. 5072–5078. doi: 10.1109/IECON.2014.7049271.

[12] M. P. Foster, J. N. Davidson, E. L. Horsley, and D. A. Stone, ‘Critical Design Criterion for Achieving Zero Voltage Switching in Inductorless Half-Bridge-Driven Piezoelectric-Transformer-Based Power Supplies’, *IEEE Trans. Power Electron.*, vol. 31, no. 7, pp. 5057–5066, Jul. 2016, doi: 10.1109/TPEL.2015.2481706.

[13] J. Forrester, J. Davidson, and M. Foster, ‘Effect of Spurious Resonant Modes on the Operation of Radial Mode Piezoelectric Transformers’, in *PCIM Europe 2018; International Exhibition and Conference for Power Electronics, Intelligent Motion, Renewable Energy and Energy Management*, Jun. 2018, pp. 1–8.

[14] J. Forrester *et al.*, ‘Equivalent circuit parameter extraction of low-capacitance high-damping PTs’, *Electron. Lett.*, Jan. 2020, doi: 10.1049/el.2019.3887.

[15] Z. Yang, J. Forrester, J. N. Davidson, M. P. Foster, and D. A. Stone, ‘Resonant Current Estimation and Phase-Locked Loop Feedback Design for Piezoelectric Transformer-Based Power Supplies’, *IEEE Trans. Power Electron.*, vol. 35, no. 10, pp. 10466–10476, Oct. 2020, doi: 10.1109/TPEL.2020.2976206.

[16] J. Forrester, J. N. Davidson, M. P. Foster, and D. A. Stone, ‘Influence of Spurious Modes on the Efficiency of Piezoelectric Transformers: a Sensitivity Analysis’, *IEEE Trans. Power Electron.*, pp. 617–629, 2020, doi: 10.1109/TPEL.2020.3001486.